06

Simulation of the interaction of accelerated electrons with an energy of $1-10\,\text{MeV}$ with a radiation-protective polymer composite

© V.I. Pavlenko, V.V. Kashibadze, A.Yu. Ruchii, S.V. Serebryakov, R.V. Sidelnikov

Belgorod State Technology University named after V.G. Shukhov, 308012 Belgorod, Russia

e-mail: artiem.ruchii.99@mail.ru Received September 25, 2024 Revised March 20, 2025

Accepted March 27, 2025

The use of physical and mathematical modeling allows us to study the processes that occur during the interaction of accelerated electrons with different energies and materials. We are considering a polymer composite based on fluoroplastic and tungsten carbide for use as biological protection in linear particle accelerator installations with electron energies up to 10 MeV. We have investigated the possibility of modifying the filler and synthesized a radiation-protective material. We have also studied the effect of accelerated electrons on the composite and determined its strength characteristics. Modifying the tungsten carbide powder allowed us to create a hydrophobic shell. The effective electron travel length in pure fluoroplastic at the energies of 1, 5, and 10 MeV is 3, 14, and 28 nm, respectively. The addition of 30 mass%The change in physico-mechanical properties of the synthesized materials was estimated. The addition of 30 mass% tungsten carbide to fluoroplast led to a 23.4% decrease in bending strength and a 16.9% increase in the two-fold filler content. The results of this work allow us to predict the behavior of composites under accelerated particle exposure and optimize their compositions to improve radiation-protective properties.

Keywords: Monte Carlo model, electron radiation, linear gas pedals, radiation-protective composite, physical and mathematical modeling.

DOI: 10.61011/TP.2025.07.61456.304-24

Introduction

The particle accelerators are devices designed to accelerate a beam of charged particles to a sublight speed and keep them at a specific orbit by means of electromagnetic fields. Since their invention, these machines can be subdivided into three types in accordance with their application: colliders designed for experiments related to the high-energy physics (HEP), accelerators of heavy ions for use in medicine and source of synchrotron radiation for detail study of applied physics [1].

Starting with 1950s, the electron accelerators provide advanced studies within the HEP and in other sciences as well. Despite the fact that the high-energy physics was a leading driving force for developing these devices, more new applications have been found for the accelerators in many fields of technologies and research. For example, progressive areas of accelerators' application include free-electron lasers, radiation therapy for cancer treatment, production of short-lived medical isotopes, beam lithography for microcircuits, synchrotron sources of light radiation, a thin-film technology and radiation processing of food products [2].

During acceleration and subsequent use of the charged particles, secondary radiation originates and it can be harmful for humans who operate and maintain the respective equipment, and for population and the environment as well [3]. Irradiation by the beams of primary particles and secondary radiation in daily work is prevented by

radiation protection surrounding the accelerator. Usually, the radiation protection material is a substance which includes atoms with large mass and charge numbers and has a significant section of hadron-nucleus interactions. A traditional material of radiation protection of the accelerators is reinforced concrete due to its comparative cheapness, strength and a capability of creating complex structures [4]. The materials for protection may also include ceramic substrates made of nitride aluminum [5,6] or polymer composites [7,8].

In the recent years, the demand for new component of the accelerators with improved operation characteristics and integrable structures such as drift tubes and internal cooling channels has encouraged research of additive production in the field of the particle accelerators [9]. The polymer-based radiation-protective materials play an important role in protection of nuclear installations, equipment and employees against harmful radiation. With new, more rigid conditions of nuclear safety, the designing of these materials has greatly changed. Scientific progress, in particular, the nanomaterial technology, makes it possible to create the radiation-protective materials that ensure great comprehensive performance [10].

Particular interest is paid to polymer composite materials (PCM) that are based on a fluoroplastic and tungsten carbide and have not only increased wear resistance and heat resistance, but excellent radiation-protection properties. The polymer-based composite materials have become ones

of the most important elements of additive production due to their improved properties and design flexibility, thereby making it possible to create components with unprecedented operation characteristics [11]. These materials are applicable in aerospace, nuclear and chemical industries, wherein they are subjected to various radiation, aggressive media and high temperatures.

Despite their excellent properties, the PCMs based on fluoroplastic and tungsten carbide can experience degradation when they are affected by ionizing radiation, in particular, accelerated electrons, especially when these materials are applied as biological protection in the linear electron accelerators [12]. It is important to understand the mechanisms of interaction of the accelerated electrons with these materials for predicting their behavior in the operating conditions and developing methods of improvement of their radiation resistance.

A useful tool for analysis of interaction of the accelerated electrons with various materials is physical-mathematical simulation. It can be used to study processes at the microscopic level and predict the behavior of the materials in various irradiation conditions. There are two models of interaction of electrons with the substance, such as a continuous slowing down approximation (CSDA) model and a Monte Carlo model.

The Monte Carlo methods are a large range of computation algorithms based on a repeated random sample for obtaining numerical values. The essence of this model is use of probability for solving specific problems. They are solved by carrying out algorithms with defined initial values and a defined system state. This method is useful when it is impossible to use other approaches. Most often, the Monte Carlo methods are used in physical-mathematical problems like simulation of transmittance of accelerated electrons through various materials, including polymers and composites based thereon [13].

The paper [14] has investigated simulation of attenuation of the proton energy in polymer films that have a protective coating made of teflon and kapton. The authors have concluded that an energy flux of ionizing radiation might be attenuated by varying a composition, a thickness and a sequence of arranged layers in the protective coating. The simulation of proton interaction has shown that at low proton energies the protection could be provided by the polymer material of the thickness of $5\,\mu\rm m$, so can at high energies by using two-layer coatings of the total thickness of about $150\,\mu\rm m$.

The study [15] has shown that in simulation of irradiation of the polymers by atomic oxygen ions with the high energy of the Kapton-H polyimide the mass loss of the latter was by an order higher than in kinetic sputtering. In turn, the acceleration coefficient during irradiation of the polymer by the high-energy ions is by two orders higher than the coefficient of acceleration of the low-energy particles.

The paper [16] presents results of simulation of interaction of electrons and protons of the 100 keV energy with volume and hollow particles of aluminum oxide. The simulation

has shown that a mean free path in the hollow particles exceeded that in the volume particles in ten times under impact of protons, so did in 2.4 times under impact of electrons.

The results of studies of the article [17] have established that irradiation by the electron flux at different temperatures substantially changes physical properties of the composite polymers. With increase of the irradiation dose, the destruction stress decreases, so does the value of bending of the material surface.

The paper [18] has analyzed impact of high-energy fast electrons on the polyimide composite that contains tungsten oxide. The calculations have shown that with increase of the content of tungsten oxide in the composite both ionization and radiation losses of the high-energy electrons increased.

The present study is aimed at designing the polymer composites based on fluoroplastic and tungsten carbide and evaluating their radiation-protective properties in relation to electron radiation with the energy from 1 to 10 MeV using the calculation models.

Materials and research methods

1.1. Initial materials

The polymer for the composite material was polytetrafluorethylene (fluoroplastic-4) as per GOST 10007-80 "fluoroplastic-4. Specifications" (by LLC "Fluoroplastic products", Belgorod, Russia). During PCM synthesis, the fluoroplastic was used as a matrix. Fluoroplastic-4 is a white press powder, whose particle size is $6-20\,\mu\mathrm{m}$. The main properties of the fluoroplastic-4 are shown in Table 1.

The radiation-protective filler was tungsten carbide (WC), which is a black powder, whose particle size is $10-250\,\mathrm{nm}$. The filler was synthesized from scraps of hard-alloy products by a unique technology described in the paper [19]. The carbon content in the compound is 8 mass%. The obtained X-ray patterns were analyzed to show that diffraction reflection of the highest intensity corresponds to tungsten monocarbide, which is presented in two crystallographic modifications: α -WC with the hexagonal lattice and β -WC with the face-centered cubic lattice [20].

1.2. Filler modification

Due to large aggregation of the filler particles, it was modified in order to create a hydrophobic shell on the material surface. Creation of this shell will allow uniform distribution of the tungsten carbide particles across the whole volume of the composite, thereby significantly reducing particle aggregation [21]. The wetting properties of tungsten carbide were changed by using the resin of K-9 of the grade "A" in accordance with a technique described in the paper [8]. The organosilicon resin is a product of condensation of methylsilanetriol and phenylsilanetriol that are produced from respective silanchlorides.

Properties	Value	Properties	Value
Density, g/cm ³	2.23	Tensile ultimate strength, kgf/cm ²	253
Melting temperature, °C	327	Elongation at fracture, %	330
Decomposition temperature, °C	415	Compression ultimate strength, kgf/cm62	125

Table 1. Basic properties of fluoroplastic-4

1.3. PCM synthesis

The powders of fluoroplastic and the WC modified filler were mixed in a mill using cryogenic grinding. The mill is provided with two grinding locations and has two different cylindrical chambers of preliminary and final grinding. The first grinding beaker contains one big steel ball, while the second beaker has several small ones. Both the chambers are closed with a cover, through which liquid nitrogen is supplied to cool the materials. The grinding was at the temperature below $-60\,^{\circ}\mathrm{C}$ with holding for 30 min.

Further on, the homogenized mixture of the powders was poured into the press form, heated to the temperature of 280 °C in a drying oven and held for 1 h. Then, the composites were pressed at the specific pressure of 80 MPa. After that, the materials were cooled down to the room temperature and sintered at the temperature of 350 °C for 3 h. Sintering of the fluoroplastic composites results in the density increase, reduction of thermal expansion and increase of thermal conductivity, which is associated with structural modifications accompanied by intensification of adhesion interphase interaction [22]. At the same time, the sintering temperature shall exceed the crystal melting temperature (327 °C), which is need to form a high degree of crystallinity (up to 90%) of the fluoroplastic samples.

1.4. Equipment used and research methods

The materials were ground and mixed using the vibration mill MM 500 NANO that is designed to use cryogenic grinding and manufactured by LLC "Kolba", Voronezh, Russia.

The semi-finished products were heated, dried and sintered using the drying oven KS-136 manufactured by LLC "Metrotrest", Neftekamsk, Russia.

The materials were pressed using the tester REM-100-A-1-1 manufactured by LLC "Metrotrest", Neftekamsk, Russia.

The bending ultimate strength tests were carried out by the equipment REM-100-A-1-1 manufactured by LLC "Metrotrest", Republic of Bashkortostan, Russia.

The crystal phases were identified using X-ray diffraction. The diffraction patterns of the powders were obtained by means of the instrument ARL X'TRA (Thermo Techno LLC, Switzerland) with a source of CuK_{α} within the angle range of 2θ from 4° to 56° . The peaks were identified by the database PDF-2 in the software packages Dif Win and Search Match.

The samples were studied by the scanning electron microscopy method (SEM) in the instrument TESCAN MIRA 3LMU (TESCAN ORSAY HOLDING, Czech Republic).

The grain size was studied by the laser light scattering particle size analyzer Analysette 22 NanoTec plus (Frisch, Idar-Oberstein, Germany) by laser diffraction in suspension. For this purpose, a small amount of the powder was solved in 96% isopropyl alcohol, since it can avoid excessive swelling of the particles, which results in distortion of the results.

The density of the studied samples was determined by hydrostatic weighing as per GOST 15139-69 (ST SEV 891-78).

Interaction of the electrons with the designed PCMs was simulated in the software CASINO V2.481 by the Monte Carlo method. The obtained results were processed by the software OriginPro V9.8.0 and Adobe Illustrator V28.7.1.

2. Results and discussion

2.1. Analysis of wettability of filler particles

The tungsten carbide was modified by the organosilicon resin K-9 to create the hydrophobic shell on the surface of the powder particles. Large change of the hydrophobic-hydrophilic balance of the filler is confirmed by the results of analysis of the contact angle of wetting. The value of the contact angle of wetting of tungsten carbide varies from $(27^{\circ} \pm 3^{\circ})$ to $(124^{\circ} \pm 4^{\circ})$.

2.2. Microscopic analysis of the synthesized PCMs

The SEM method was taken to study the composites that were synthesized using the non-modified and modified filler in order to confirm efficiency of modification on WC distribution in the polymer and their aggregation. Fig. 1 shows the SEM images of the WC composites using modification and without it. The dark area of the SEM images is an area of distribution of the polymer (fluoroplastic), the light area is the filler.

It is seen that modification of the filler significantly contributed to prevention of aggregation of the particles and more uniform distribution across the whole volume of the composites. In doing so, use of the cryogenic grinding when mixing the fluoroplastic powder with the non-modified WC had almost no effect on the size of

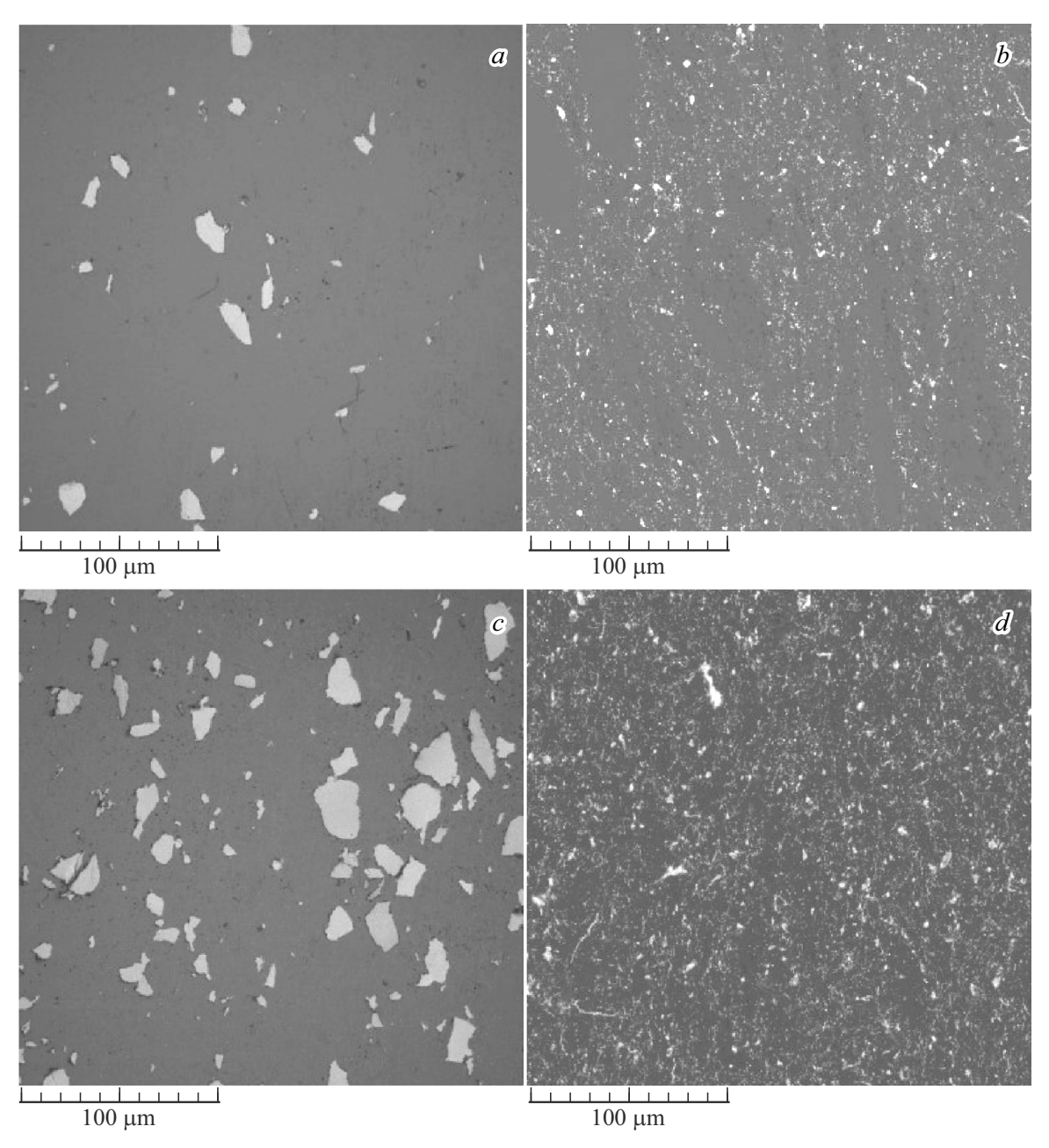


Figure 1. SEM images of the composites with the content of 30 mass% (a, b) and 60 mass% WC (c, d): a, c — non-modified; b, d — modified.

the aggregated particles of the filler. The sizes of agglomerates of the WC powder particles and the sizes of WC agglomerates in the composite (Fig. 1,a,c) are up to $20\,\mu\text{m}$. Most likely, this is due to the fact that the WC powder has a quite small size of the particles up to a nanoscale level, wherein the Van der Waals forces start to act between the particles, and they have enough energy and can not be destroyed even during cryogenic grinding.

We note that the use of modification could exclude agglomeration of the WC powder particles, whereas the cryogenic grinding is effecting when mixing the fluoroplastic with WC.

2.3. Physical and mechanical characteristics of the PCMs

The density of the produced composites with a different content of the modified WC was determined at a 10%-step by hydrostatic weighing. First of all, the weight of the composite in air was determined, and so after that was it in the liquid with a known density (distilled water). After weighing the samples in air and liquid, the density was found by the formula:

$$\rho = \frac{m}{m - m_1} \cdot \rho_w,\tag{1}$$

Concentration WC, mass% 0 10 20 30 40 50 60 70 80 Density, g/cm³ 2.05 2.23 2.45 2.70 3.02 3.43 3.96 4.68 5.73

Table 2. Density of the radiation-protective composites with the various content of the modified WC

where m — the composite weight in air; m_1 — the composite weight in water; $\rho_w = 0.998 \,\mathrm{g/cm^3}$ — the density of distilled water at 20°C.

The obtained results of the density of the composites are shown in Table 2. Introduction of the fillers significantly increases the density of the composites, since WC has a higher density (16.63 g/cm³) as compared to the fluoroplastic. Thus, with increase of the WC content to 30 mass% the variation of the composite density increased by 31.7%, and with increase of the WC content to 60 mass%— it increased by 93.2%.

The mechanical properties of the composite materials under impact of a bending load were studied using the standard technique GOST R 57749-2017 (ISO 17138:2014) There were 5 tests for each composition. The distance between the supports was 14-15 mm, the maximum load of the experiment was 598 N. The three-point bending strength (MPa) was calculated by the formula

$$\sigma_{f,m} = \frac{3F_m \cdot L}{2b \cdot h^2},\tag{2}$$

where F_m — the maximum load, [N]; L — the distance between the lower supports, [mm]; b — the sample width, [mm]; h — the average sample thickness, [mm].

The composite samples were synthesized, and they contain 30 mass% and 60 mass% of the modified WC powder. Besides, in order to evaluate introduction of the filler into the composite composition, for comparison the samples made of pure fluoroplastic were manufactured. Fig. 2 shows the curves of the bending strength dependence of the studied composites depending on the fill degree. Based on the obtained data, a regression curve was constructed taking into account the confidence interval of 95%. The highest bending strength belongs to the samples without the filler ((27.8 ± 2.0) MPa). With increase of the content of the modified WC to 30 mass%, the strength characteristics evaluated by the bending strength are reduced to (21.3 ± 1.5) MPa (Fig. 2), while with further increase (to 60 mass%) there is insignificant increase ((23.1 \pm 1.6) MPa). This may be attributed to the fact that during strength evaluation of the highly-filled composite there is a starting role of not only a bond of the polymer with the filler, but of the strength of the filler itself. Since WC has high physical-mechanical properties, then it is more difficult to destroy the composite with 60 mass% of the solid powder, which increases the strength properties of the composite as a whole.

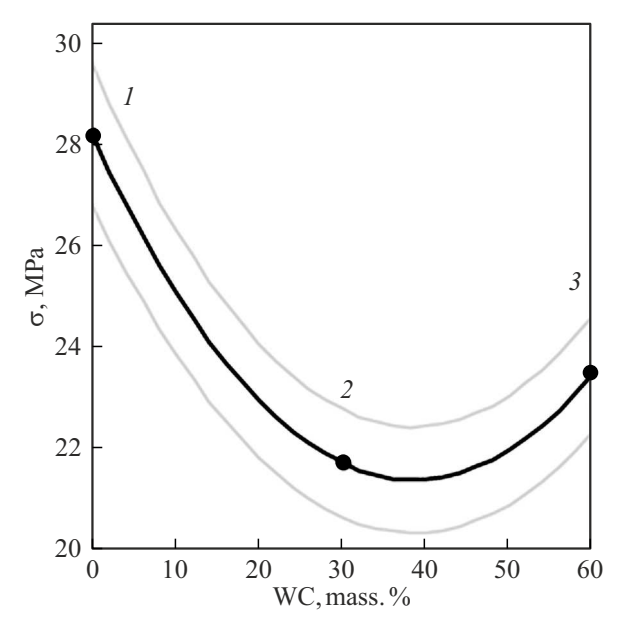


Figure 2. Curves of the dependence of bending strength of the studied composites depending on the WC fill degree: 1 — the fluoroplastic, 2 — the composite with WC 30 mass%, 3 — the composite with WC 60 mass%.

2.4. Physical-mathematical simulation of interaction of the accelerated electrons with the PCMs

Transmittance of the electrons with the energies from 1 to $10\,\mathrm{MeV}$ through the designed polymer radiation-protective composites was simulated based on an elemental chemical composition of the composites. The specified energy range (from 1 to $10\,\mathrm{MeV}$) is attributed to the fact that the bulk of the application linear electron accelerators has the energy of the electron beams up to $10\,\mathrm{MeV}$, whereas the most promising energy range of the electron beam for creating the continuous conductive electron accelerators with high power is considered to be $1-5\,\mathrm{MeV}$ [23,24].

The theoretical calculations were performed for the sample made of the pure fluoroplastic and for the composites containing 30 mass% and 60 mass% of WC. The atomic elementary composition of the studied materials is shown in Table 3. The simulation did non take into account compounds of the substances used in modifications due to their small (less than 1%) contribution.

During transmittance through the substance, the electrons at the low energies $(E < 1 \, \text{MeV})$ lose their energy primarily due to ionization. Since the rate of ionization losses grows

Maria	Content in the material, mass%			
Material	W	С	F	
Fluoroplastic	0.0	24.0	76.0	
Composite containing 30 mass% simulation WC	28.2	18.6	53.2	
Composite containing 60 mass% simulation WC	56.4	13.2	30.4	
rithmically with increase of the energy, the losses of eleration radiation grow almost linearly (the portion all the losses negligible depends on the energy) and minate over the critical energy by several tens of MeV the most materials [25].	— for the flucture $\left(-\frac{dE}{dx}\right)$	$= \rho_C \frac{Z_C}{A_C} F(E_K),$		
he ionization losses of the electron energy in the		$+\rho_F \frac{-F}{A_F} F(E_K,$	I_F), [MeV/cm],	

Table 3. Atomic elementary composition of the studied materials for simulation

logai dece of a dom for t

Tł studied radiation-protective composites were calculated by the following formula [26]:

$$\left(-\frac{dE}{dx}\right)_{ion} = K\rho \frac{Z}{A} \cdot \frac{1}{2\beta^2} \left[\ln\left(\frac{m_e c^2 E_k}{I^2} \cdot \frac{\beta^2}{2(1-\beta^2)}\right) - (2\sqrt{1-\beta^2} - 1 + \beta^2) \ln 2 + 1 - \beta^2 + \frac{1}{8}(1 - \sqrt{1-\beta^2})^2 \right], \text{ [MeV/cm]},$$
(3)

where the index "ion" means losses for collision of the particles with the atoms, A — the atomic mass of the element, [g/mol], Z — the atomic number (the serial number of the element in the periodic table), $K = 4\pi r_e^2 m_e c^2 N_A =$ = 0.307 MeV/(g/cm²), $m_e c^2 = 0.511$ MeV — the electron rest energy, $r_e = \frac{e^2}{m_e c^2} = 2.8 \cdot 10^{-13} \, \text{cm}$ — the classic electron radius, $N_A = 6 \cdot 10^{23} \, \text{mol}^{-1}$, ρ — the substance density, [g/cm³], I — the average ionization potential of the medium substance atom, [eV], $\beta = \sqrt{1 - \frac{(m_e c^2)^2}{(m_e c^2 + E_k)^2}}$ — the Lorentz factor of the electron with the kinetic energy E_k .

Since the considered radiation-protective composites are a mixture of several atoms of various chemical elements, it is necessary to use a composition Bragg law: the mixture or compound can be regarded as being composed of thin layers of pure elements in the respective proportion (Bragg additivity). In this case, it is possible to find the losses by the following formula:

$$\frac{dE}{dx} = \sum \omega_j \frac{dE}{dx_j}, \text{ [MeV/cm]}, \tag{4}$$

where $\frac{dE}{dx_j}$ — the average rate of the energy loss in the j-th

Using the composition Bragg law (4), the ionization losses of the electron energy were calculated by the formulas:

$$\left(-\frac{dE}{dx}\right)_{ion} = \rho_C \frac{Z_C}{A_C} F(E_K, I_C) + \rho_F \frac{Z_F}{A_F} F(E_K, I_F), \text{ [MeV/cm]},$$
 (5)

— for the composite material with WC:

$$\left(-\frac{dE}{dx}\right)_{ion} = \rho_C \frac{Z_C}{A_C} F(E_k, I_C) + \rho_F \frac{Z_F}{A_F} F(E_k, I_F)$$
$$+\rho_W \frac{Z_W}{A_W} F(E_k, I_W), \text{ [MeV/cm]}, \tag{6}$$

where

$$F(E_k, I) = \frac{K}{2\beta^2} \left[\ln \left(\frac{m_e c^2 E_k}{I^2} \cdot \frac{\beta^2}{2(1 - \beta^2)} \right) - (2\sqrt{1 - \beta^2} - 1 + \beta^2) \ln 2 + 1 - \beta^2 + \frac{1}{8} (1 - \sqrt{1 - \beta^2})^2 \right].$$
 (7)

The radiation losses of the energy with transmittance of the electrons through the designed radiation-protective composites were determined using the following formula:

$$\left(-\frac{dE}{dx}\right)_{rad} = \rho \, \frac{Z^2}{A} \cdot \frac{K\alpha}{4\pi} \cdot \frac{\varepsilon}{m} \cdot G(E_k), \text{ [MeV/cm]}, \quad (8)$$

where $\varepsilon = E_k + m_e c^2$ — the full electron energy, [MeV]; $\alpha = \frac{1}{137}$ — the fine structure constant.

$$G(E_k) = \frac{K\alpha}{4\pi} \cdot \frac{\varepsilon}{m} \cdot \left[\frac{12\varepsilon^2 + 4m_e^2 c^4}{3\varepsilon p} \ln\left(\frac{\varepsilon + p}{m_e c^2}\right) - \frac{(8\varepsilon + 6p)m^2 c^4}{3\varepsilon p^2} \cdot \left(\ln\left(\frac{\varepsilon + p}{m_e c^2}\right)\right)^2 - \frac{4}{3} + \frac{2m^2 c^4}{\varepsilon p} \cdot F\left(\frac{2p(\varepsilon + p)}{m^2 c^4}\right) \right], \tag{9}$$

where $F(x) = F\left(\frac{2p(\varepsilon+p)}{m^2c^4}\right) = \int_0^{\frac{2p(\varepsilon+p)}{m^2c^4}} \frac{\ln(1+y)}{y} dy$, p — the electron momentum, [g·cm/s].

Using the composition Bragg law (the formula (4)), the radiation losses in the studied radiation-protective composites were calculated by the following formulas:

— for the fluoroplastic:

$$\left(-\frac{dE}{dx}\right)_{rad} = \left(\rho_C \frac{Z_C^2}{A_C} + \rho_F \frac{Z_F^2}{A_F}\right) G(E_k), \text{ [MeV/cm]},$$
(10)

— for the composite material with WC:

$$\left(-\frac{dE}{dx}\right)_{rad} = \left(\rho_C \frac{Z_C^2}{A_C} + \rho_F \frac{Z_F^2}{F} + \rho_W \frac{Z_W^2}{A_W}\right) \times G(E_k), \text{ [MeV/cm]}.$$
(11)

The total (summed) losses of the electron energy with transmittance through the radiation-protective composite materials were calculated by the following formula:

$$\left(-\frac{dE}{dx}\right) = \left(-\frac{dE}{dx}\right)_{rad} + \left(-\frac{dE}{dx}\right)_{ion}, \text{ [MeV/cm]}. (12)$$

Fig. 3 shows the curves of the ionization and radiation losses of the electron energy as well as the total losses of the electron in the fluoroplastic and the composites containing WC. The simulation has been done for the energy of the electrons from 1 to 10 MeV.

For all the considered energies of the electrons, the contribution of the ionization losses significantly exceeds the contribution of the radiation losses to the total losses of the electrons both in the fluoroplastic and in the composites containing WC. The least total losses of the electron are observed when simulating transmittance through the pure fluoroplastic without fillers, so are the greatest ones with transmittance through the composite containing WC as the filler (60 mass%).

Introduction of the large content of the WC filler from 30 mass% to 60 mass% into the radiation-protective composite materials based on the fluoroplastic results in increase of both the ionization and the radiation losses of the fast electrons.

It is known that the larger contribution to the total losses of the electron energy is provided by the atoms of heavy elements in comparison with the atoms having the small serial numbers in the periodic table [27,28].

It is known that with transmittance through the material the fast electrons experience multiple scattering, so their path in the substance is not straight (as for the heavy particles). Their motion path changes repeatedly, and only some electrons of the beam pass over the maximum distance in the material in a direction perpendicular to its surface.

As a result of scattering (deceleration) of the electrons in the electric field with transmittance through the substance, deceleration radiation originates. Since the deceleration radiation is much stronger for lighter particles, then this effect is more important for the electrons than for the protons, alpha-particles and the heavy charged nuclei (fission fragments). This effect may be neglected with the particle energy below 1 MeV, since the energy losses due to deceleration radiation are very small. The losses for radiation begin to be significant only with the particle energies that significantly exceed the minimum energy of ionization. At the relativistic energies, the ratio of the loss rate in deceleration radiation to the loss rate in ionization is approximately proportional to a product of a kinetic energy of the particle and the atomic number of the absorber.

In this regard, there is scientific interest of simulating transmittance of the electrons through the composites not only by evaluating the total losses of the electron energy, but their visual path as well as origination of deceleration radiation.

Transmittance of electron radiation with the energy from 1 to 10 MeV was simulated by using simulation by means of the Monte Carlo method in the software CASINO V2.481 [29]. The mentioned program uses tabulated elastic interaction cross sections (Mott) and experimentally determined decelerating forces to calculate the paths of electrons in the substance [30]. The program is designed to plot the path of motion of electrons and to calculate an effective travel length of electrons in the specified composite material. The initial data for the software are a density and an atomic composition of the material.

The total number of the emitted simulated particles of electrons was 1000 in the software. All the electrons started their motion from one point that was adjacent to the material. Fig. 4 graphically depicts the paths of motion of the electrons in the studied materials and variation of the kinetic energy in motion. It is seen that when simulating irradiation by the electron beam the bulk of the electrons in the material does not keep a direction of motion of the primary beam of the fast electrons. It is clear that the path of the electrons consists of portions that are determined by a distance between two consecutive acts of elastic scattering during an atom collision. In all the studied materials, the path of the electron motion after scattering becomes so complicated that it looks like a process of diffusion of particles in the substance. The absolute depth of penetration of the electrons in the fluoroplastic and the WC composite turns out to be much less than the full path of the electron before deceleration, which is defined by the ionization and radiation losses.

The mass of the electrons is significantly less than the mass of the heavy particles, thereby affecting the nature of their motion in the substance. In collisions with the atom electrons and the nuclei, the electrons significantly deviate from the original direction of motion and travel along a winding path. Therefore, there is a notion of an effective travel length for the electrons, which is defined by the minimum thickness of the substance that is measured along the initial speed of the beam and corresponds to full absorption of the electrons.

Fig. 5 shows the curves that demonstrate the dependence of the effective electron travel length in the fluoroplastic and the radiation-protective WC composites on the initial kinetic energy.

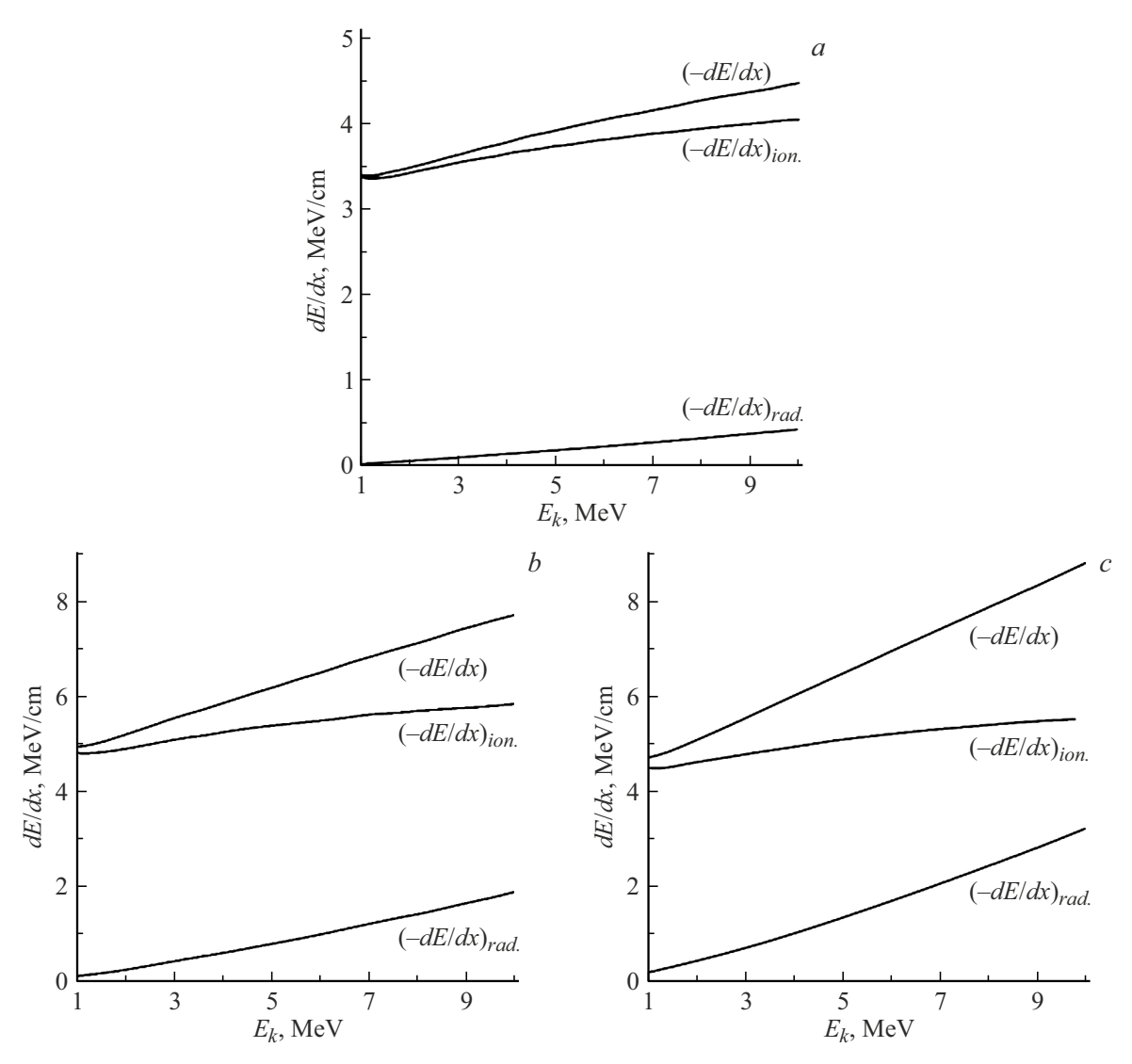


Figure 3. Curves of the dependence of the energy losses of the fast electrons on the initial E_k in the following materials: a — the fluoroplastic, b — the composite with WC 30 mass%, c — the composite with WC 60 mass%.

Table 4 shows the data for the effective (average) electron travel length in the fluoroplastic and the radiation-protective WC composites depending on the initial kinetic energy of the electrons in comparison with the known analogues. The effective electron travel lengths in iron and concrete were found using the data of the paper [31].

The main factors governing the radiation protection materials are the cost and space availability. With significantly large space restriction, the main emphasis is placed not on the cost, but rather the thickness of protection.

Originally, either a concrete chamber or a metal wall was used for radiation protection of the industrial electron accelerators [34]. Concrete is the most suitable and cost-effective and it shall be used wherever it is possible. It can be poured into a pre-defined formed and it has excellent mechanical properties. In radiation therapy installations, the typical concrete barriers can vary from 60 cm (the secondary barriers) to 2 m (the primary barriers) of common concrete.

The accelerators of higher energy and power may require a significantly larger thickness, but it also heavily depends on the distances, on radiation sources in living quarters and, therefore, on the size of the radiation room. In places where the space is restricted, it is possible to use baryte fillers or iron-containing aggregates such as ilmenite magnetite [35].

The data for the effective electron travel length have been analyzed to show that with increase of the electron energy the effective travel length significantly increases (Table 4). For the pure fluoroplastic without fill, with increase of the initial kinetic electron energy from 1 to 5 MeV, the effective electron travel length increases in 4.85 times, while with increase of the initial kinetic electron energy from 1 to 10 MeV it increases in 9.70 times. For the composite with a filler of tungsten carbide of 30 mass%, with increase of the initial kinetic electron energy from 1 to 5 MeV, the effective electron travel length increases in 6.08 times, while with increase of the initial kinetic electron energy from 1 to

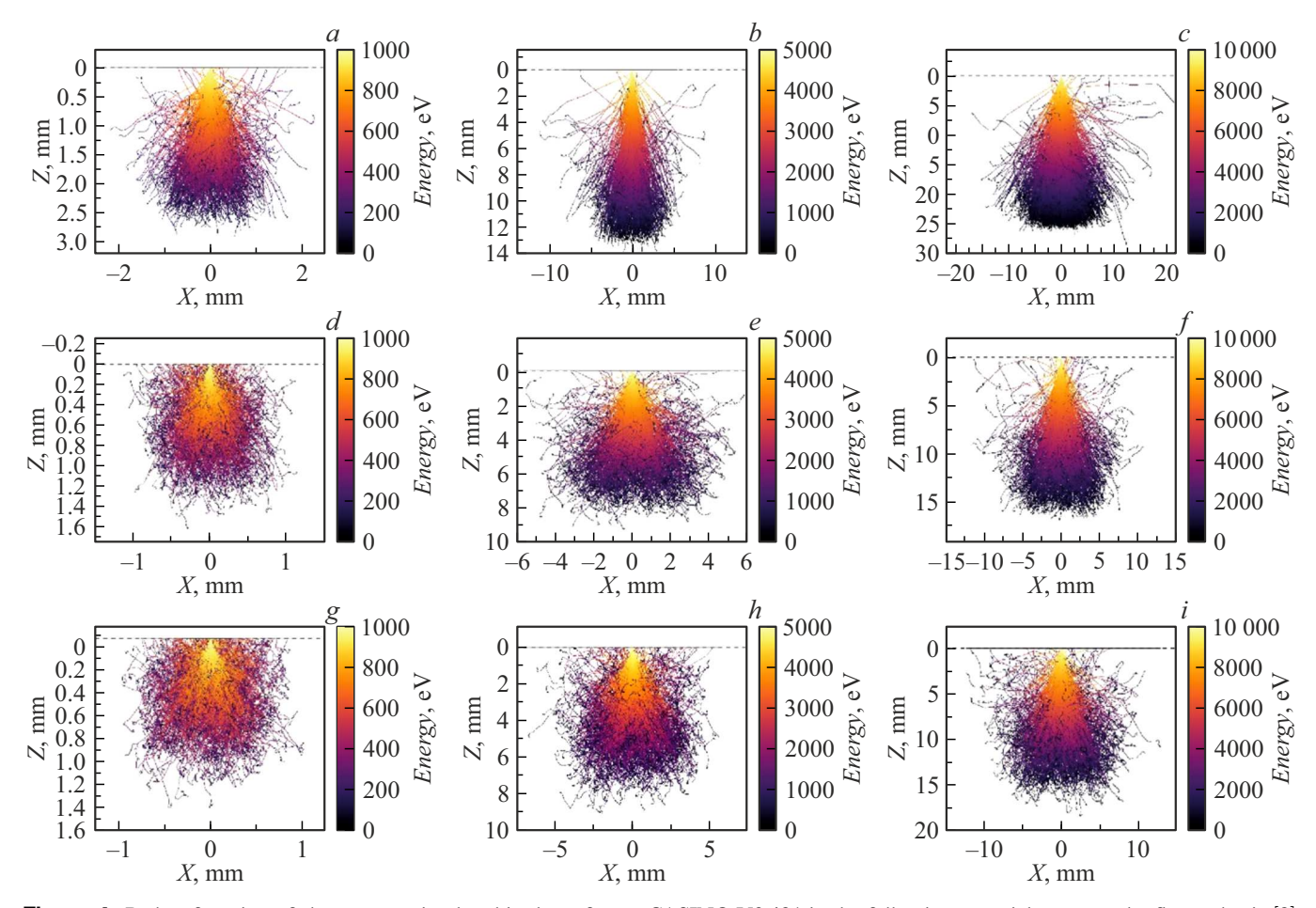


Figure 4. Paths of motion of electrons as simulated in the software CASINO V2.481 in the following material: a-c — the fluoroplastic [8]; d-f — the composite with WC fill of 30 mass%; g-i — the composite with WC fill of 60 mass%; with the following initial energies of the electrons: a, d, g — 1 MeV, b, e, h — 5 MeV, c, f, i — 10 MeV.

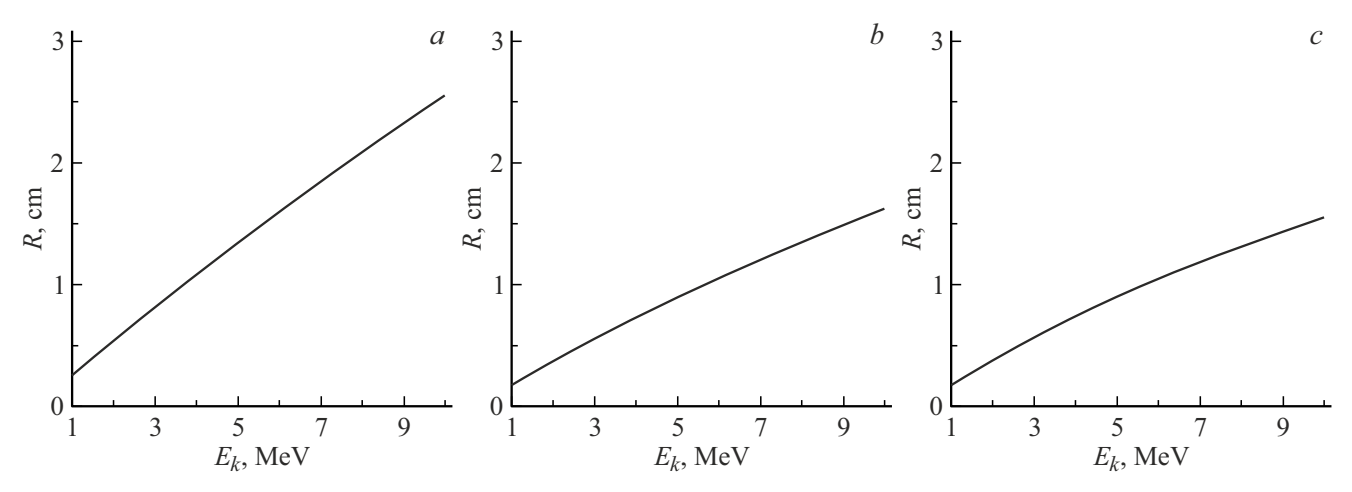


Figure 5. Curves of the dependence of the effective electron travel length on the initial E_k in the following materials: a — the fluoroplastic, b — the composite with WC 30 mass%, c — the composite with WC 60 mass%.

10 MeV it increases in 13.23 times. For the composite with filler of WC 60 mass%, with increase of the initial kinetic electron energy from 1 to 5 MeV, the effective electron travel length increases in 6.25 times, while with increase

of the initial kinetic electron energy from 1 to 10 MeV it increases in 14 times.

It can be seen that filling with the proposed filler (WC) significantly reduces the effective electron travel length in

Material	Effective electron travel length, mm			
iviateriai	1 MeV	5 MeV	10 MeV	
Fluoroplastic	2.7	13.1	26.2	
The composite containing 30 mass% WC (the density 2.7 g/cm ³)	1.3	7.9	17.2	
The composite containing 60 mass% WC (the density 4.0 g/cm ³)	1.2	7.5	16.8	
Iron (the density 7.9 g/cm ³)	0.8	4.2	7.7	
Concrete (the density 2.3 g/cm ³)	2.2	12.8	24.4	
KM-1* (the density 3.8 g/cm ³)	1.6	7.9	_	
Polyimide composite filled with bismuth silicate Bi ₁₂ SiO ₂₀ (the density 2.95 g/cm ³) [32]	2.3	10.2	_	

Table 4. Effective electron travel length in the studied materials and their analogues

Note*: The composite material containing finely-dispersed activated-modified oxides Fe₂O₃ and Bi₂O₃ and duralumin as a binder [33].

the composites as compared to the pure fluoroplastic in the initial conditions of simulation. Thus, with simulation of transmittance of the electrons with the initial kinetic energy of 1 MeV, there is observed reduction of the effective electron travel length by 51.85% with filling with 30 mass% of tungsten carbide in comparison with the pure fluoroplastic. With the greatest initial kinetic energy of 10 MeV of simulation, there is observed reduction of the effective electron travel length by 35.88% with filling with WC 60 mass% in comparison with the pure fluoroplastic.

Thus, introduction of the proposed filler significantly reduces the effective travel length of electron transmittance within the entire studied range of the electron energies. Reduction of the effective travel length will allow significantly reduce the thickness of the radiation protection of the linear electron accelerators, which is especially important for modernization of the existing operating electron accelerators.

The comparative analysis of the average range of the electrons in the designed composites and the existing analogues (Table 4) has shown that in terms of the average range of the electrons the proposed radiation-protective composites exceed such materials as common concrete, KM-1 and the polyimide composite filled with bismuth silicate Bi₁₂SiO₂₀, being only inferior to iron. Bu the iron density is 7.9 g/cm³, while the density of the composites is in at least two times less than that (depending on the composition). Besides, the main problem of protection against the fast electrons is reduced to protection against secondary deceleration radiation, while with increase of the density of the material the intensity of deceleration radiation multiply increases. So, it can be concluded that the designed composites in a complex exceed the existing analogues in terms of protection against electron radiation at the considered energies from 1 to 10 MeV.

3. Conclusion

- 1. The PCMs have been synthesized based on the fluoroplastic press powder and the modified WC.
- 2. It is experimentally confirmed that the WC modification resulted in the change of hydrophobic-hydrophilic balance of the surface of its surface, wherein introduction of the modified filler into the fluoroplastic matrix significantly reduces aggregation of the filler particles.
- 3. The physical-mechanical tests of the synthesized PCMs have been performed. The highest bending strength belongs to the samples without the filler and is 27.8 MPa. With the content of 30 mass% of the modified WC in the composite, the strength characteristics evaluated by the bending strength are reduced by 23.4% and are 21.3 MPa. At the same time, if the content of the filler is increased to 60 mass%, then there is observed insignificant increase of the strength characteristics of the material by 8.45% in comparison with the 30 mass% additive. It is also determined that the composites with the WC additive have a high density.
- 4. The calculation of the ionization and the radiation losses of the electron energy has shown that the contribution of the former is significant in all the composites. The least losses of the energy are observed for the additive-free sample, while addition of the modified radiation-protective filler results in increase of the total losses of the energy of the fast electrons.
- 5. Interaction of the accelerated electrons with the energy of $1-10\,\mathrm{MeV}$ with the designed polymer composite has been simulated. Filling with the proposed filler (WC) significantly reduces the calculated effective electron travel length in the composites as compared to the pure fluoroplastic in the initial conditions of simulation. Thus, when introducing WC $30\,\mathrm{mass\%}$ into the fluoroplastic matrix, the effective electron travel length decreases by $51.9\,\%-34.4\,\%$. When

adding 60 mass% of the filler into the polymer, the effective electron travel length has been reduced by 55.6%-35.9% in comparison with the additive-free composition. The further research will be aimed at experimental studies of irradiating the designed composites in the linear accelerators of the electrons with the energy of up to $10\,\text{MeV}$ in order to confirm their radiation-protective properties and the developed theoretical models.

Funding

This study was supported by the grant No. 24-79-10033 from the Russian Science Foundation, https://rscf.ru/project/24-79-10033/. Equipment provided by the High-Technology Center of the Belgorod State Technology University named after V.G. Shukhov was used in experiments.

Conflict of interest

The authors declare that they have no conflict of interest.

References

- [1] Vikas, R. Sahu. Precis. Eng., **71**, 232 (2021). DOI: 10.1016/j.precisioneng.2021.03.015
- [2] J. Resta Lopez. Future Particle Accelerators (IntechOpen, London, 2022), DOI: 10.5772/intechopen.106340
- [3] G. Haridas, R. Ravishankar, A. Chattaraj, P. Selvam. Hand-book on Radiation Environment, 2, 263 (2024). DOI: 10.1007/978-981-97-2799-5_10
- [4] G.N. Timoshenko. *Radiatsionnaya zashchita vysokoener-gitichnykh uskoritelei* (OIYaI, Dubna, 2022) (in Russian).
- [5] Y.P. Severgin, M.Z. Filimonov. Proceed. Intern. Conf. Particle Accelerators, 3, 2208 (1993).DOI: 10.1109/PAC.1993.309270
- [6] A. Kozlovskiy, I. Kenzhina, Z.A. Alyamova, M. Zdorovets. Opt. Mater., 91, 130 (2019). DOI: 10.1016/j.optmat.2019.03.014
- [7] C.V. More, Z. Alsayed, M.S. Badawi, A.A. Thabet, P.P. Pawar. Environ Chem. Lett., 19, 2057 (2021).
 DOI: 10.1007/s10311-021-01189-9
- [8] V.I. Pavlenko, G.G. Bondarenko, V.V. Kashibadze, S.N. Domarev. Perspektivnye materialy, 7, 42 (2024) (in Russian). DOI: 10.30791/1028-978X-2024-7-42-50
- [9] T. Romano, G. Pikurs, A. Ratkus, T. Torims, N. Delerue, M. Vretenar, L. Stepien, E. López, M. Vedani. Phys. Rev. Accel. Beams, 27, 1 (2024). DOI: 10.1103/PhysRevAccelBeams.27.054801
- [10] C. Zeng, Q. Kang, Z. Duan, B. Qin, X. Feng, H. Lu, Y. Lin. J. Inorg. Organometall. Polymers Mater., 33 (8), 2191 (2023). DOI: 10.1007/s10904-023-02725-6
- [11] E. McCarthy, D. Brabazon. In: Encyclopedia of Materials: Composites, ed. by D. Brabazon (Oxford, Elsevier, 3, 2021, 263). DOI: 10.1016/B978-0-12-819724-0.00067-7
- [12] A. Passarelli, M.R. Masullo, Z. Mazaheri, A. Andreone. Sensors, 24, 5036 (2024). DOI: 10.3390/s24155036
- [13] A.A. Jaoude. Recent Advances in Monte Carlo Methods (IntechOpen, London, 2024), DOI: 10.5772/intechopen.1000269
- [14] I.V. Verkhoturova (Gopienko), M.S. Bykovskii, A.V. Avrashenko, K.K. Tyazhelkova. Vestnik AmGU, 81, 28 (2018) (in Russian).

- [15] V.A. Shuvalov, N.A. Tokmak, N.I. Pis'mennyi, G.S. Kochubei. Pribory i tekhnika eksperimenta, 4, 79 (2021) (in Russian). DOI: 10.31857/S0032816221040108
- [16] V.Yu. Yurina, V.V. Neshchimenko. V sb.: Fizika: fundamental'nye i prikladnye issledovaniya, obrazovanie, pod red. A.I. Mazura (TOGU, Khabarovsk, 2022), s. 90–92 (in Russian).
- [17] B.A. Kozhamkulov, Zh.M. Bitibaeva, Zh.E. Primkulova, D.E. Kuatbaeva, A.K. Dzhumadillaeva. Sci. Eur., 50-1 (50), 18 (2020) (in Russian).
- [18] N.I. Cherkashina. Tech. Phys., 65 (1), 107 (2020).DOI: 10.1134/S1063784220010028
- [19] A. Galuga, G. Baravov, V. Gavrish, S. Smirnov, A. Losenkov, S. Vostrognutov. Method and device for obtaining a powder from particles of tungsten or tungsten compounds with a size in the nano-, micron or submicron range (European Patent NºEP3138932A1, 08.03.2017)
- [20] I.Kh. Khudaykulov, J.R. Ravshanov, Kh.B. Ashurov, V.N. Arustamov, D.T. Usmanov. J. Surf. Investig: X-Ray Synchrotron Neutron Tech., 16 (4), 599 (2022). DOI: 10.1134/S1027451022040280
- [21] V.I. Pavlenko, G.G. Bondarenko, N.I. Cherkashina. Inorganic Mater.: Appl. Res., 11 (2), 304 (2020).
 DOI: 10.1134/S2075113320020306
- [22] N.I. Cherkashina, V.I. Pavlenko, A.N. Shkaplerov, A.A. Kuritsyn, R.V. Sidelnikov, E.V. Popova, L.A. Umnova, S.N. Domarev. Adv. Space Res., 73 (5), 2638 (2024).
 DOI: 10.1016/j.asr.2023.12.003
- [23] D.S. Yurov, V.I. Shvedunov, A.S. Alimov. Moscow University Phys. Bull., 78 (1), 85 (2023).
 DOI: 10.55959/MSU0579-9392.78.2310501
- [24] O.V. Tkhorik, V.A. Kharlamov, I.V. Polyakova, N.N. Loy, M.G. Pomyasova, V.I. Shishko. RUDN J. Agron. Anim. Ind., 18 (4), 541 (2023).
 DOI: 10.22363/2312-797X-2023-18-4-541-553
- [25] D.F. Crawford, H. Messel. *Electron-photon shower distribution function* (Elsevier Science, 2013, Berlin)
- [26] V.I. Bespalov. Vzaimodeistvie ioniziruyushchego izlucheniya s veshchestvom: uch. posobie (Tomskii politekh. un-t, Tomsk, 2008) (in Russian).
- [27] V.I. Pavlenko, G.G. Bondarenko, N.I. Cherkashina. Perspektivnye materialy, **8**, 5 (2015) (in Russian).
- [28] A.V. Pavlenko, N.I. Cherkashina, R.N. Yastrebinski, A.V. Noskov. Problems Atom. Sci. Technol., 111 (5), 21 (2017).
- [29] D. Drouin, A.R. Couture, D. Joly, X. Tastet, V. Aimez, R. Gauvin. Scanning, 29 (3), 92 (2007). DOI: 10.1002/sca.20000
- [30] P. Hovington, D. Drouin, R. Gauvin. Scanning, 19 (1), 1 (2006). DOI: 10.1002/sca.4950190101
- [31] M.J. Berger, J.S. Coursey, M.A. Zucker, J. Chang. Stopping-power and range tables for electrons, protons, and helium ions (NIST PML, Gaithersburg, 2017), DOI: 10.18434/T4NC7P
- [32] N.I. Cherkashina, V.I. Pavlenko, A.V. Noskov. Radiat. Phys. Chem., 159 (1), 111 (2019).
 DOI: 10.1016/j.radphyschem.2019.02.041
- [33] Yu.M. Samoilova. Avtoref. kand. diss. (Belgorod, BGTU im. V.G. Shukhova, 2015) (in Russian).
- [34] V.V. Krayushkin, P.A. Orlenko, A.V. Larichev. Atomnaya energiya, (in Russian). 61 (3), 218 (1986).
- [35] W.P. Swanson. Radiological safety aspects of the operation of electron linear accelerators international atomic energy agency (IAEA, Vienna, 1979)

Translated by M.Shevelev